Polymer Testing 117 (2023) 107832

Contents lists available at ScienceDirect

Polymer Testing

journal homepage: www.elsevier.com/locate/polytest

Self-healing materials based on disulfide bond-containing acrylate networks

L.M. Sáiz [a,*], M.G. Prolongo [b], V. Bonache [a], A. Jiménez-Suárez [a], S.G. Prolongo [a]

[a] Materials Science and Engineering Area, Escuela Superior de Ciencias Experimentales y Tecnología, Universidad Rey Juan Carlos, C/ Tulipán s/n, 28933, Móstoles, Madrid, Spain

[b] Materials and Production Aerospacial, Politechnic University, Plaza Del Cardenal Cisneros, 3, 28040, Madrid, Spain

ARTICLE INFO

Keywords:
Self-healing
Disulfide bonds
Acrylate
Vitrimers

ABSTRACT

Disulfide containing vitrimers are being widely studied to get renewable, reprocessable and self-healable resins. The most of them are based on thermally cured epoxy resin. Herein, new thermoset systems based on typical acrylate monomers with photo-curing were synthesized with self-healing capabilities by introducing monomers with disulfide bonds. These disulfide groups are able to exchange upon heating, leading to a renewal of the crosslinks across the damaged surfaces. Different ratios of associative reversible exchange covalent bonds have been studied. The samples were evaluated in terms of thermal and mechanical properties. It was found that the glass transition temperature (Tg) is lower than that corresponding to typical acrylate thermosets, but mechanical properties are better. Increases in hardness of 2.4 times and in elastic modulus of 1.7 times with respect to the reference networks were achieved.

Finally, the self-healing properties of the disulfide acrylates were demonstrated by monitoring the repair of a scratch upon heating. A new experimental test for quantifying the self-healing efficiency has been optimized, following the recovery of the surface crack by perfilometry. The composition optimization allows us to achieve repair percentages of 95% in shorter times.

1. Introduction

Photo-curable resins with functional properties are playing an important role for industrial applications, due to the environmental advantages, fast curing, high production efficiency and low energy consumption. In addition, the possibility of handling the reaction and the final product through the combination of several parameters (type and concentration of de initiator, the intensity of the light, temperature, and the monomer structure), gives an additional advantage. Moreover, the photocurable resins are widely used as feedstock for 3D printing polymer manufacture, due to their fast-curing reaction, which can be locally applied layer by layer. This has led to high rise in demand for new photocuring resins with high performance and new functionalities [1,2].

Acrylate photocuring systems are widely used in coatings [3], 3D printing [4,5] or dental materials [6], where a control of the polymerization is needed. However, the rapid photopolymerization reaction cause an early increase in the viscosity of the resin and the gel point can be reached in advance. As a result, an internal polymerization stress is induced, and a large volume shrinkage is generated. The shrinkage stress generated during polymerization can lead to the formation of microcracks and deformation of the material, as well as delamination from or warping of the substrate as stress is transferred to the interfaces of the material [7–10]. This volume shrinkage will be detrimental to their performance and durability and increases the expected probability of failures and the associated costs of repair and maintenance. The generated microcracks are a huge problem on thermosetting coatings and films, which main function is environmental protection of the substrate due to their corrosion resistance is seriously decreased.

Several methods have been investigated to limit the amount of shrinkage stress that develops during polymerization, such as: the use of composite materials [11–15], adjusting the molecular weight and the bulkiness of the monomers [11,12], altering the cure protocol [16–18].

However, an alternative to extend their service life would be the use of self-healing materials. Self-healing polymers are representative examples of smart materials, capable of repairing themselves after being exposed to one or several external stimuli such as chemicals, heat, moisture, or light [19,20]. Several methods to obtain healable polymers can be found in literature, depending on whether they require or not an

* Corresponding author.
E-mail address: luciana.saiz.moritan@urjc.es (L.M. Sáiz).

https://doi.org/10.1016/j.polymertesting.2022.107832
Received 27 April 2022; Received in revised form 5 September 2022; Accepted 9 October 2022
Available online 10 October 2022

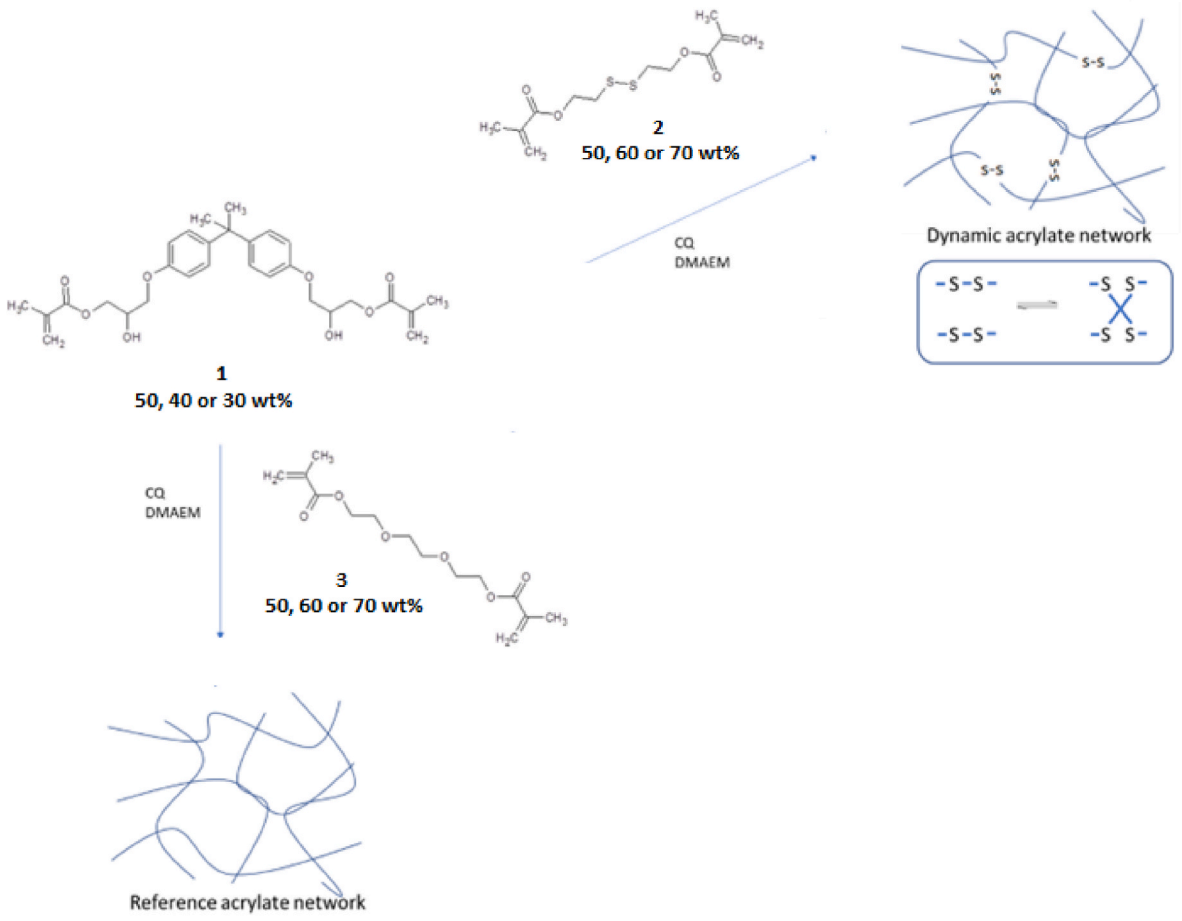

Fig. 1. Synthesis of dynamic and reference acrylate networks.

external repair agent, respectively. The main advantages of the latter, where self-healing is achieved by the material itself through its chemical nature, are that the properties of the material do not change when the self-repair is made, and also that they can be repaired an unlimited number of times [21].

An attractive chemical strategy to introduce self-healing in crosslinked polymer networks is offered by the introduction of reversible or dynamic chemical bonds. These types of bonds have ability to break and reform between several molecules under the action of an external stimulus. Polymers networks containing such exchangeable bonds are also known as Covalent Adaptable Networks (CANs), as such materials can adapt their macromolecular architecture in response to an external stimulus or trigger, despite their crosslinked nature [22]. These molecular rearrangements provide a microscopic mechanism for achieving macroscopic flow and stress relaxation without risking structural damage or permanent loss of the material properties [23,24].

One of the most commonly used links in the design of materials with reversible covalent bonds is the dynamic disulfide bond. Disulfide bonds can reversibly cleave, reform, and exchange under certain conditions and the response of the material can be adjust using different crosslinkers and varying the amount of the disulfide bonds present in the final material.

These disulfide bonds have been extensively studied in epoxy resins with thermal curing, to obtain self-healing materials [24–28], however this type of bonds have not been applied in acrylic resins. Taking as reference the classic acrylate system based on Bisphenol A bis (2-hydroxyl-3-methacryloxypropyl)ether (Bis-GMA) and triethyleneglycol dimethacrylate (TEGDMA), in this work the TEGDMA is replaced by a similar monomer with disulfide bond in its structure. The goal is to obtain a functional material with reversible bonds in order to extend the service life. On the other hand, other challenge was also addressed in this work is the development of experimental test to measure quantitatively the self-healing efficiency of surface cracks. In the bibliography, the most of published papers show photographs and/or optical micrographs of the cracks before and after the healing treatment. We have optimized a quantitative analysis procedure.

2. Materials and methods

2.1. Materials

The resins were formulated from blends of Bisphenol A bis(2-hydroxyl-3-methacryloxypropyl)ether (Bis-GMA, Eschem) and Bis(2-methacryloyl)oxyethyl disulfide (DISULFIDE-GMA, Aldrich) at mass fractions of 50:50, 40:60 and 30:70.

Blends of Bisphenol A bis(2-hydroxyl-3-methacryloxypropyl)ether (Bis-GMA) and triethyleneglycol dimethacrylate (TEGDMA, Eschem) were used as reference of samples without disufide bonds. Bis-GMA (1), DISULFIDE-GMA (2) and TEGDMA (3) were used as received.

The resins were activated for visible light polymerization by the addition of 0.7 wt% camphorquinone, (CQ, Aldrich) in combination with 0.32 wt% of dimethylamino ethylmethacrylate (DMAEMA, Aldrich) in order to accelerate the polymerization of the blend.

Fig. 1 shows a scheme of the proposed systems. Both are similar, the main difference is the presence of reversible disulfide bonds. For it, different combination of DISULFIDE-GMA (2) and TEGDMA (3) are used to optimize the final thermosetting formulation with high performance and self-healing ability.

The light source employed was assembled from a UV chamber (Otoflash G171) with a maximum spectral distribution between 400 and

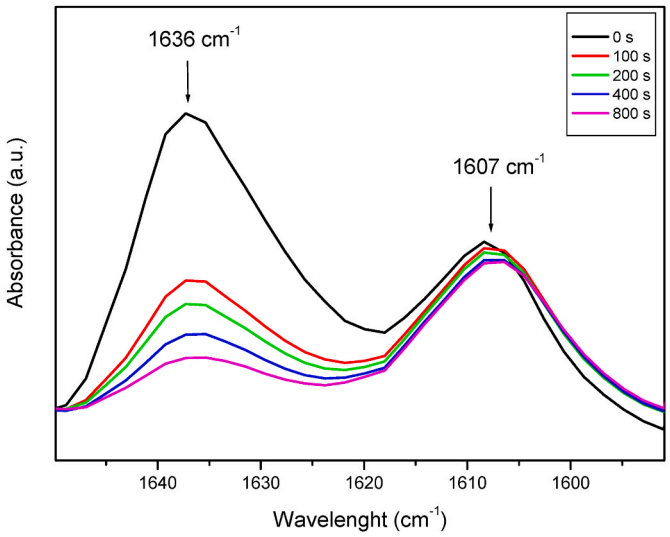

Fig. 2. FTIR spectra of double bonds for Bis-GMA/DISULFIDE-GMA 50:50 wt% sample as a function of the irradiation time.

500 nm. The light source was selected in order to obtain an optimum overlap between the spectral irradiance of the curing unit and the absorption spectrum of CQ.

2.2. Methods

Fourier transform infrared (FTIR) spectra were acquired with a Nicolet 6700 Thermo Scientific. Mid-infrared (MIR) spectra were acquired over the range 4000-600 cm^{-1} from 16 co-added scans at 2 cm^{-1} resolution. The resins were spread out on KBr windows and were irradiated at regular time intervals and spectra were collected immediately after each exposure interval. The double bond conversion (DC) was calculated from equation (1), following the decay of the absorption band located at 1636 cm^{-1} (A_{1636}) corresponding to C═C and using the absorption of phenyl ring at 1607 cm^{-1} (A_{1607}) as reference.

$$DC = \left[1 - \frac{A\ 1636/A1607\ cured}{A1636/A1607 uncured}\right] \quad \text{equation 1}$$

Dynamic mechanical thermal analysis (DMTA V Rheometric Scientific instrument) measurements were done in dual cantilever bending mode at 1 Hz and strain of 0.1%, with temperature increasing from 30 to 250 °C at 2 °C.min^{-1}. The dimensions of the specimens were:35 × 11 × 1mm^3. The glass transition of the acrylate networks was taken at the maximum in tan δ-temperature curves.

An optical 3D perfilometer (Zeta Instruments, Phoenix, AZ, USA) was used to study the healing process of the samples before and after a thermal treatment.

Hardness ando Young's Modulus were evaluated by nanoindentation by means of a MTS Nano Indenter XP using a pyramidal Berkovich tip. Ten tests were carried out at room temperature on each material, using XP quasi static mode and applying a load of 10 mN.

3. Results

3.1. Measurement of the double bond conversion (FTIR)

To ensure maximal curing degree on the new proposed thermosetting resins, the conversion of the carbon double bonds as a function of irradiation time was determined [30]. Methacrylate conversion of monomers was assessed by FTIR spectroscopy. Samples were irradiated at consecutive irradiation intervals, and after each exposure interval

Table 1
Maximum double bond conversion (%DC) reached for the samples with disulfide bonds after photo and thermal curing.

% DC	50:50	40:60	30:70
Photocuring	80.3	77	78.5
Thermal post-curing	84.8	86.1	88.1

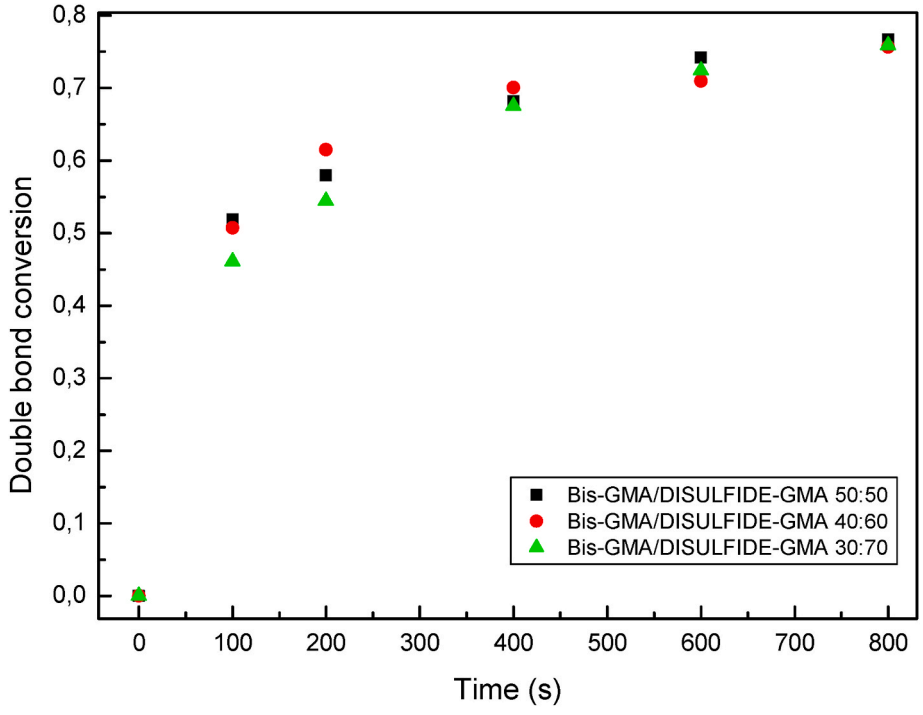

Fig. 3. Monomer conversion versus irradiation time measured by FTIR.

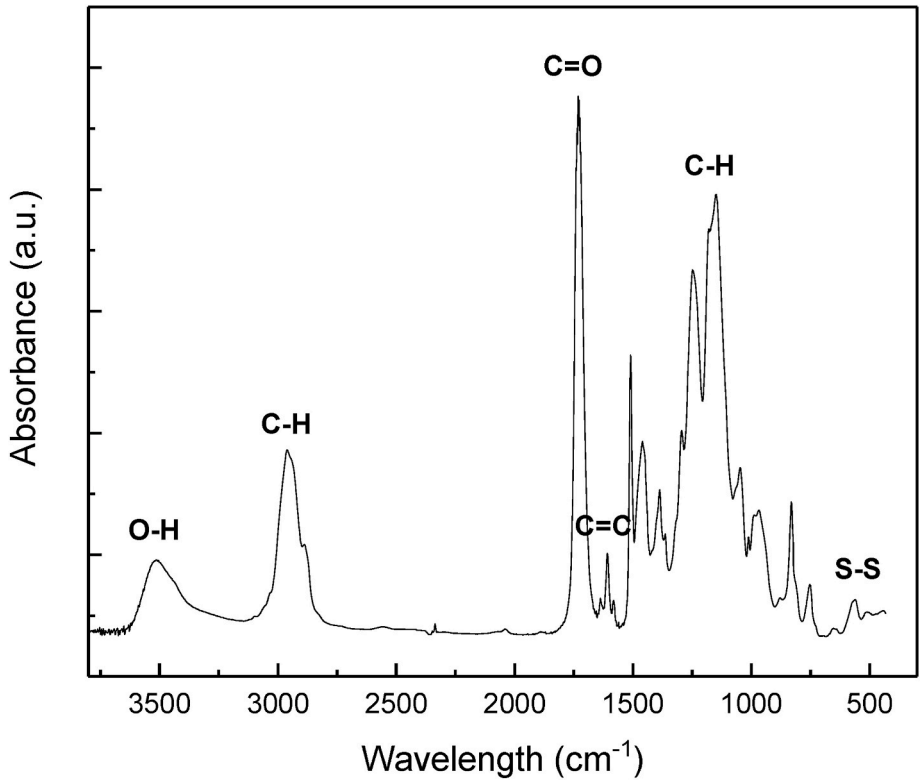

Fig. 4. Representative FTIR spectra of a post-cured Bis-GMA/DISULFIDE-GMA 50:50 wt% sample.

mid-infrared (MIR) spectra were collected. Representative spectra are displayed in Fig. 2.

The conversion of methacrylate groups was calculated from the decay of the band located at 1636 cm^{-1} which is associated with the C═C stretching vibrations. Fig. 3 shows the conversion as a function of the exposure time to visible light for the different blends. The degree of cure reached after visible exposure was calculated according to Eq. (1). Table 1 collects the maximum conversion reached for each composition. As it can be seen, no composition reaches complete conversion, this behavior agrees to what is expected for acrylate systems, where the maximum conversion obtained is about 70%. As the disulfide content increases, the curing reaction rate is lightly lower, but the maximum conversion reached is the same for all the studied samples.

After the photopolymerization, the samples were thermally post-cured in an oven at 140 °C for 2 h and was monitored by FTIR spectroscopy. The conversion reached in the thermal postcuring was calculated according to eq (1) and the values are collected in Table 1.

After the thermal treatment, the overall conversion of the methacrylate groups advanced to around 84–88%, depending on the composition of the sample. This behaviour is due to the activation of the reactive species that remained alive when the sample was devitrified. Higher conversions were achieved in systems with a higher monomer content of DISULFIDE-GMA, because these mixtures have greater mobility due to the flexibility of this monomer compared to the rigid aromatic BISGMA [31,32].

Representative FTIR spectra of a post-cured Bis-GMA/DISULFIDE-GMA 50:50 wt% sample is shown in Fig. 4. The characteristic peaks at 3500 cm^{-1} could be assigned to O–H stretching vibration. The peaks between 2970 and 2870 cm^{-1} are attributed to the aliphatic C–H stretch of the matrix. The characteristic peak of the carbonyl C = O bond of Bis-GMA and DISULFIDE-GMA appeared at 1730 cm^{-1}. The double carbon bonds C═C bonds at 1607 cm^{-1} and 1582 cm^{-1} corresponded to the aromatic chains. The absorption peaks at 1460 cm^{-1} are present due to skeletal vibrations of aromatic rings. Out-of-plane bending vibration modes of aromatic C–H bonds are observed at 1299, 1255, 1179, 1038 cm^{-1}. The absorption peaks observed below 1000 cm^{-1} illustrated in-plane-bending vibration modes of C–H bonds. The presence of disulfide bonds is verified by weak bands between 560 and 510 cm^{-1}.

3.2. Thermal analysis (DMTA)

The Tg of the post-cured samples could not be readily discerned by DSC, probably due to a wide transition (as will be later confirmed by DMTA) and with a possible small change in enthalpic capacity. Therefore, DMTA experiments were carried out. The DMTA curves in terms of loss factor (tan δ) for the materials subjected to the additional thermal post-curing treatment are shown in Fig. 5. It can be seen the appearance of broad peaks reflects that the acrylate matrix behaves mechanically as no homogeneous, that is, there are regions with high mobility that relax at lower temperatures and rigid regions that relax at higher temperature. As tan δ, is a ratio of viscose (dissipation of the energy due to segmental movements, friction and heat) to elastic (reversible deformation) response, the sharp and high tan δ peak of the samples containing lower content of DISULFIDE-GMA, indicates a significant increase in friction in the sample, and high energy is transformed into heat in a short temperature range, therefore it reflects the higher homogeneity of this sample. The smooth shape of the tan δ curves for samples with higher DISULFIDE-GMA content indicates a progressive molecular mobility as temperature increases meaning that the material can absorb energy continuously from lower temperatures.

Tg values of 135, 139 and 170 °C were observed for DISULFIDE-GMA contents of 50, 60 and 70 wt% respectively, to what could indicate a higher crosslinking degree with the highest disulfide content.

On the other hand, the reference samples were also analyzed and Tg values of 190, 191 and 192 °C (Fig. 5b) were observed for TEGDMA contents of 50, 60 and 70 wt% respectively. The Tg of the samples with DISULFIDE-GMA shows higher flexibility with enhanced chain movement compared to the reference ones. Moreover, narrower peaks are observed for the reference samples, which would indicate that these samples are more homogeneous. This may be also enhanced by the

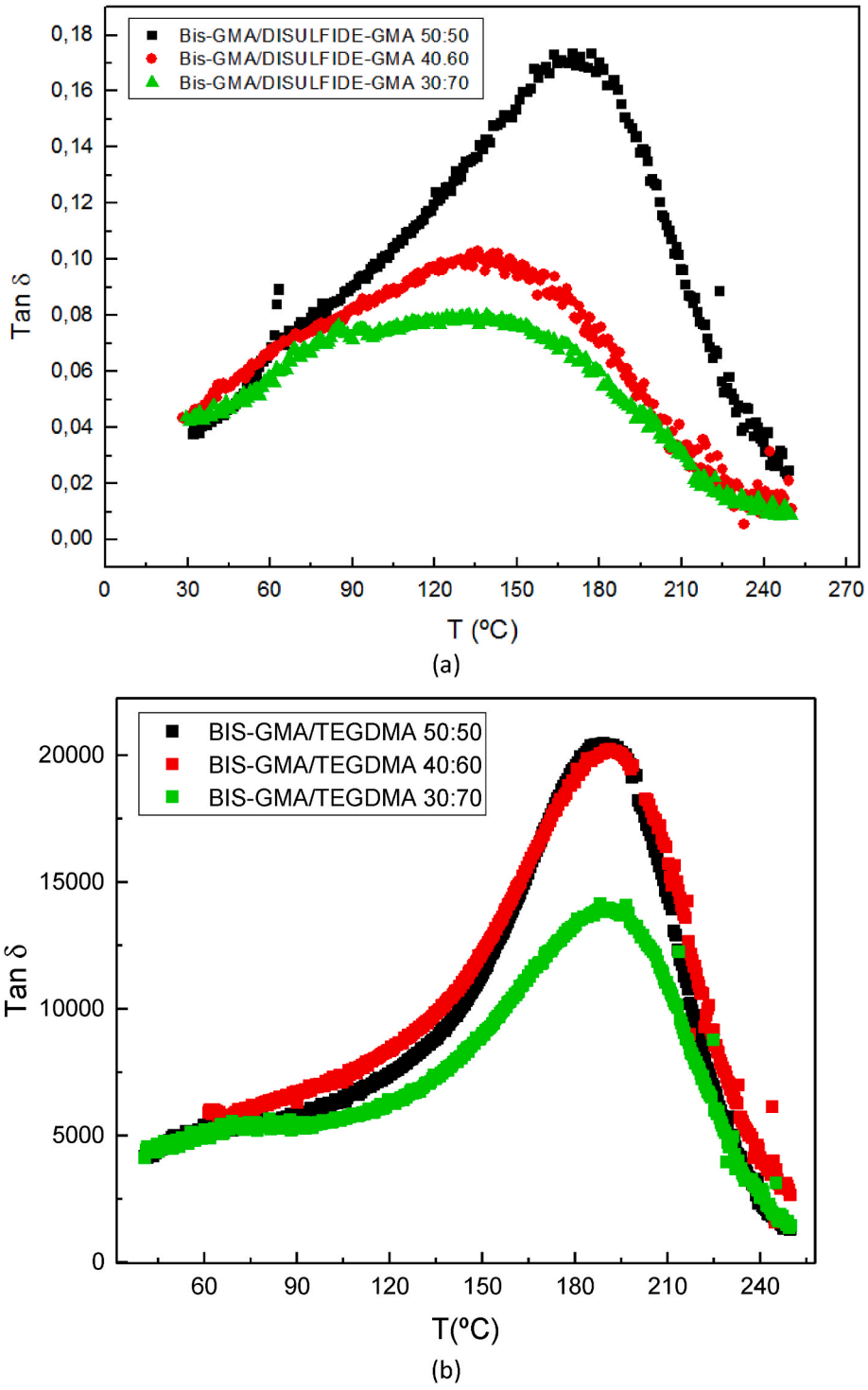

Fig. 5. DMTA curves for post-cured samples.

hydrogen bonds between the hydroxyl groups of BISGMA and the oxygen atoms of TEGDMA, compared to the sulfur atoms of DISULFIDE-GMA.

In all the samples the tan δ′ temperature curves (see Fig. 5a) showed a shoulder in the range 50–80 °C which corresponds to a small drop in E′-temperature curves. This is a β-relaxation that appears in others crosslinked poly(methyl methacrylate)s [33].

The storage modulus (E′) value of all compositions showed an abrupt reduction above the glass transition temperature, due to the movement of the chains and the dissipation of mechanical energy attributed to the relaxation of the network. As expected, the storage modulus presents at big drop in the glass transition zone. The storage modulus (E′) in the glassy state (E'_G) was taken at 80 °C (T < Tg) and in the rubbery state (E'_R) was taken at 220 °C T > Tg).

In the glassy state, all the samples have similar E'_G (~0.8 GPa), independently of the composition, as it is typical of the glassy state. Looking to E'_R in the rubbery state, there was no significant differences for 60-40 and 50-50 samples (70 MPa). However, E'_R for the sample having 70% DISULFIDE-GMA reached a higher value (270 MPa) which is a clear evidence of the higher density of crosslinking (more than three

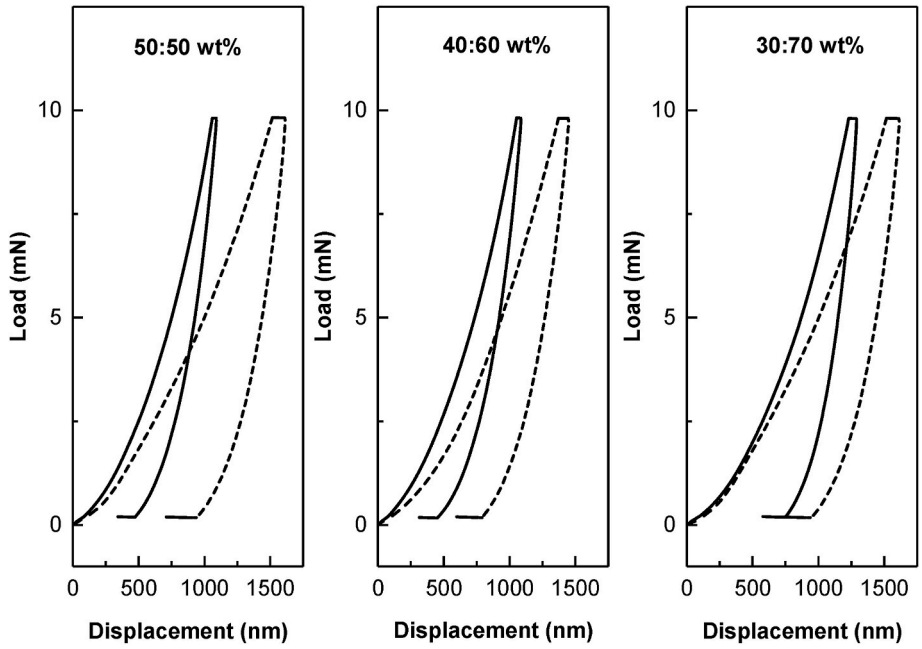

Fig. 6. Characteristic loading-pause-unloading vs penetration depth of the disulfide (solid line) and reference (dash line) acrylate networks.

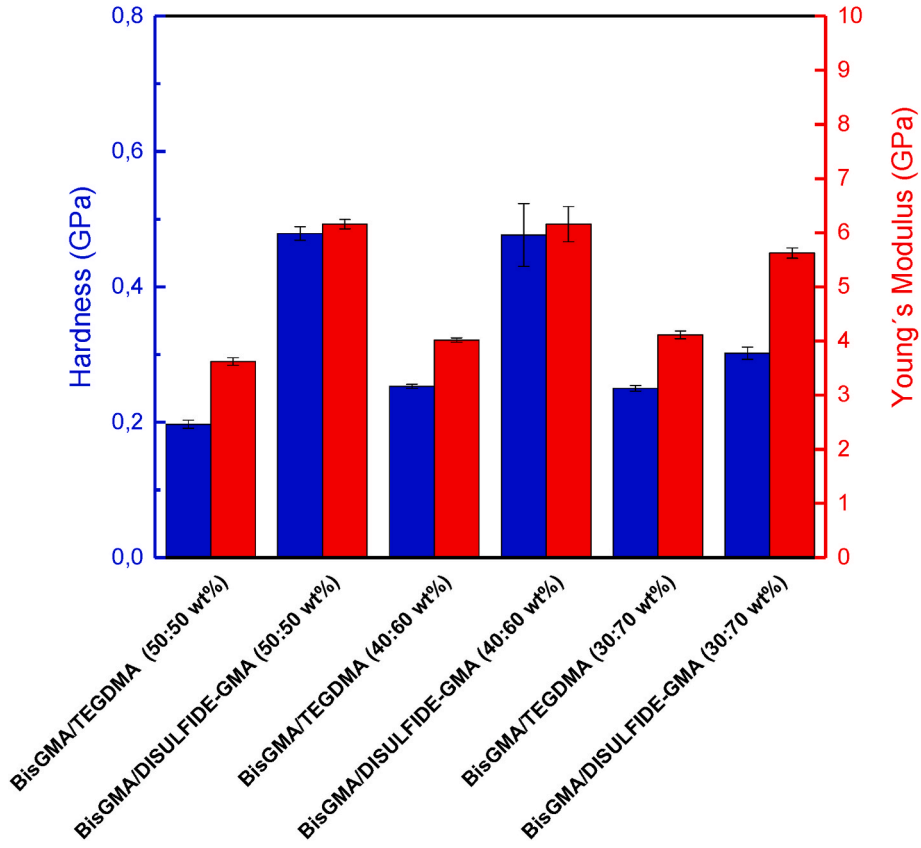

Fig. 7. Comparison of hardness and elastic modulus for the formulations with and without disulfide bonds.

times).

For a polymer network, the storage modulus value in the rubbery plateau region is correlated with the number of crosslinks. Specifically, the elastic modulus of a polymer network above Tg increases as increase in the crosslinking density (ν). From the theory of rubber elasticity [34], the crosslink density of a polymer network can be calculated from the shear modulus (G) in the rubbery region (T > Tg). For an incompressible network (E = 3G), allowing calculate the crosslinking density from equation (2):

$$\nu = G/RT = E_R RT/3 \quad (2)$$

where: ν = cross-linking density (mol.cm^{-3}); E_R = elastic storage

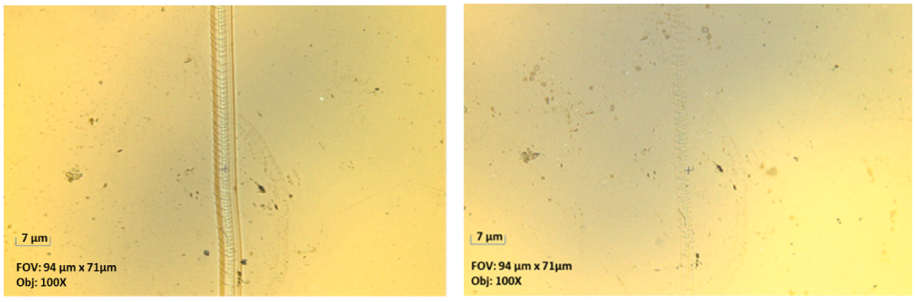

Fig. 8. Images of the damage zone before (a) and after (b) the thermal treatment at 140 °C for 180 min for Bis-GMA/DISULFIDE-GMA 50:50 wt% sample.

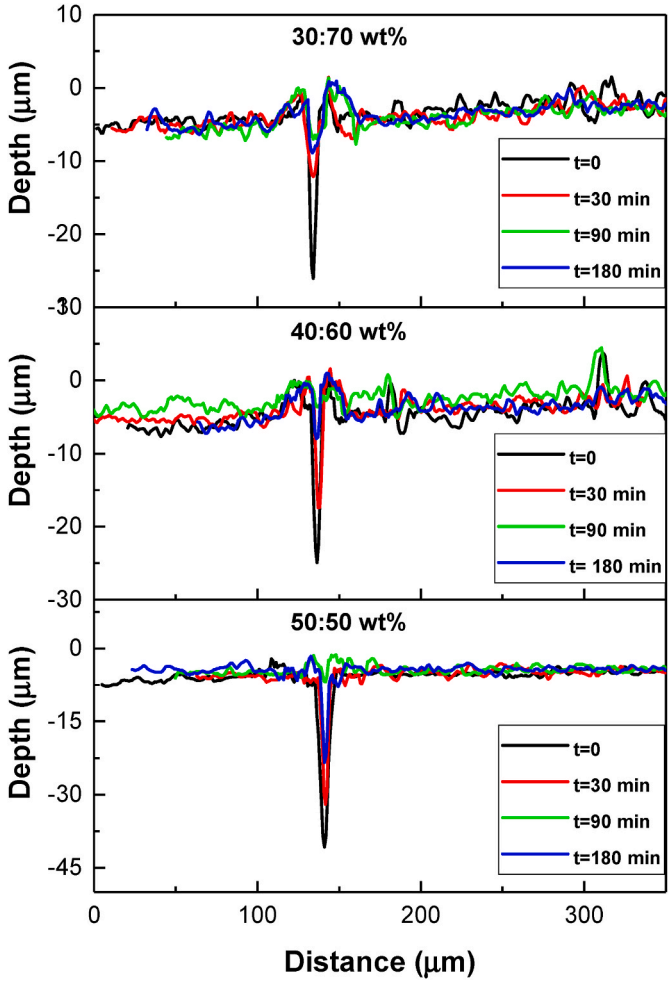

Fig. 9. Evolution of the scratch depth during thermal treatment at 140 °C.

modulus in the rubbery region; R = the universal gas constant (J.mol^{-1}.K^{-1}) and T = absolute temperature (K).

From the E'$_R$ (220 °C) the cross-linking density results are 6·10^{-3} mol cm^{-3} for the samples containing 50% and 60% of DISULFIDE-GMA, and 22·10^{-3} mol cm^{-3} for the sample having 70% of DISULFIDE-GMA. This means that a threshold of disulfide bonds is required for the effective exchanged S–S reaction.

Table 2
Healing behavior of the samples as a function of the amount of the DISULFIDE-GMA.

Time	Healing ratio (HR%) 50:50	Healing ratio (HR%) 40:60	Healing ratio (HR%) 30:70
t = 0	0	0	0
t = 30 min	33	33	65
t = 90 min	42	88	85
t = 180 min	94	94	95

3.3. Nanoindentation analysis

In order to determine possible mechanical properties changes of samples with disulfide bonds with respect to the typical BISGMA-TEGDMA acrylates systems, nanoindentation tests were performed. Nanoindentation is a widely used technique for the determination of nanomechanical properties and specially to get information on alterations in the structure of thermosetting resins [29]. Typical load-displacement curves are shown in Fig. 6. From the load-depth curves, mechanical properties such as the elastic modulus and the hardness, can be calculated and compared (Fig. 7). Fig. 7 indicates that the presence of DISULFIDE-GMA increases both hardness and elastic modulus at room temperature for all the compositions when compared with the reference resin. Increases in hardness of 142, 85 and 26% for monomer disulfide contents of 50, 60 and 70 wt % respectively, were obtained with respect to the reference samples. A similar behavior was obtained for the elastic module, where increases of 70, 34 and 26% were obtained with respect to the references. A possible explanation for this finding may be sought in the rather flexible nature of TEGDMA in comparison to DISULFIDE-GMA at room temperature. Additionally, the mechanical properties of the reversible network at room temperature did not change with the increasing of disulfide bonds content in the acrylate resin, which was important for potential industrial applications due to its properties was not affected. In this way an acrylic resin was endowed with special self-healing properties by replacing the normal resin with the dynamic acrylic resin.

In addition, the influence of the experimental ratio on the hardness was analyzed. It was observed a decrease in the hardness when comparing the sample with 50% of DISULFIDE-GMA with respect to the one content 70%. DISULFIDE-GMA is a linear flexible aliphatic monomer while BISGMA is a rigid aromatic monomer, for that reason it is expected that as the amount of the flexible monomer increases, the hardness of the sample decrease.

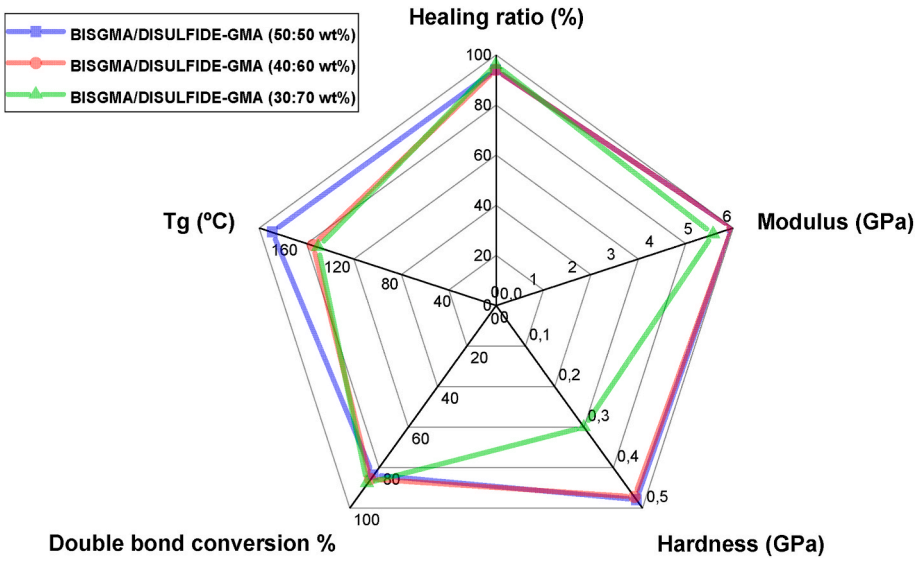

Fig. 10. Overall networks performance with the different disulfide compositions related to the material testing results.

3.4. Thermal healing behaviour

Due to the exchangeable disulfide reaction, the acrylic resin has the ability of self-healing under external stimuli. First, the evaluation of thermal triggered healing ability was performed on a film of the sample. Fig. 8.a shows a micrograph of a scratched sample before the heating process. Then the film was heated for 180 min at 140 °C. The micrograph of the healed sample is shown in Fig. 8.b. As it is seen there the scratch was significantly reduced meanwhile the surrounding region remain unchanged.

A quantitative analysis of the thermal healing behavior was carried out by a perfilometric analysis of the samples before and after the thermal treatment, in order to confirm the self-healing performance. Fig. 9(a–c) show a profile of the scratch as function of thermal treatment.

To determine the influence of the disulfide concentration on the self-healing properties, several polymers were prepared using different weight fractions of BISGMA and DISULFIDE-GMA. Initially, a scratch of 20–30 μm was performed on the samples. Table 2 shows the healing ratio in function of the amount of the disulfide bond. It can be observed that as the content of the DISULFIDE-GMA monomer increases, the recovery is faster. However, after 180 min an almost complete recovery of the scratch was observed in all the samples, indicating that an excellent healing degree was attained.

Moreover, it is expected that at higher temperatures there will be greater mobility of the chains and therefore the regeneration of the disulfide bonds will occur more quickly and therefore the self-healing also.

However, samples without disulfide groups, does not show any self-healing property at all, indicating that the healing behavior was not cause by a photo-thermal softening of the material.

For a better indication of the overall acrylate disulfide networks performance, the material properties of all the samples related to quantitative experimental results is additionally given in the form of radar chart in Fig. 10. These systems have the possibility of adjusting the composition to maximize mechanical behavior or self-healing capacity, according to the desired application. In cases where it is necessary to achieve a repair in shorter times, improving the mechanical properties with respect to the reference matrix, materials with high disulfide bonds contents will be chosen. On the contrary, if it is necessary to obtain materials with higher Tg values and mechanical properties, regardless of the time required to raise the maximum repair, materials with lower disulfide bonds contents will be chosen.

4. Conclusions

New novel photocurable acrylate polymers containing disulfide bonds were successfully synthesized. The presence of the disulfide bond allowed us to activate an efficient thermal-induced healing of the material, reaching recovery values up to 95%. In addition, the time required to reach it is a function of the content of the disulfide groups present in the final material. This healing effect is attributed to the exchange reaction of the disulfide bonds upon heating, leading to a renewal of the crosslinks across the damaged surfaces.

On the other hand, a remarkable increase in hardness and elastic modulus is noticed compared to typical acrylate systems for all the formulations developed. Increases up to 2.4 times in hardness and 1.7 times in the elastic moduli were achieved with respect to similar networks without disulfide bonds.

Finally, these systems have the possibility of adjusting the composition to maximize mechanical behavior or self-healing capacity, according to the desired application.

Therefore, these experimental results will serve as a basis for extending the life of acrylate materials and expanding their scope of application.

Author statement

L. M. Sáiz: Conceptualization; Formal analysis; Methodology; Visualization; Writing – original draft. **M. G. Prolongo:** Supervision, Formal analysis, Writing – review and editing. V. Bonache: Formal analysis; Methodology. Alberto Jiménez-Suárez: Supervision; Writing – review and editing. Silvia G. Prolongo: Supervision; Writing – review and editing.

Declaration of competing interest

The authors declare that they have no known competing financial interests or personal relationships that could have appeared to influence the work reported in this paper.

Data availability

Data will be made available on request.

Acknowledgements

This paper has received funding from the European Union's Horizon 2020 research and innovation programme under the Marie Sklodowska-Curie grant agreement Nº 754382 and Young Researchers R&D Project (Ref. M2183, SMART-MULTICOAT) financed by Universidad Rey Juan Carlos and Comunidad de Madrid.

References

[1] X. Wang, M. Jiang, Z. Zhou, J. Gou, D. Hui, 3D printing of polymer matrix composites: a review and prospective, Compos. B Eng. 110 (2017) 442–458. https://doi:10.1016/j.compositesb.2016.11.034.
[2] W. Gao, Y. Zhang, D. Ramanujan, K. Ramani, Y. Chen, C.B. Williams, C.C.L. Wang, Y.C. Shin, S. Zhang, P.D. Zavattieri, The status, challenges, and future of additive manufacturing in engineering, Comput. Des. 69 (2015) 65–89. https://doi:10.1016/j.cad.2015.04.001.
[3] Ying Wang, Rongjun Qu, Yuankai Pan, Yuexin Luo, Ying Zhang, Changmei Sun, Chunnuan Ji, High-performance UV-curable epoxy acrylate nanocomposite coatings reinforced with aramid nanofibers, Prog. Org. Coating 163 (2022), https://doi.org/10.1016/j.porgcoat.2021.106631.
[4] J. Guit, M.B.L. Tavates, J. Hul, C. Ye, K. Loos, J. Jager, R. Folkersma, V.S.D. Voet, Photopolymer resins with biobased methacrylates based on soybean oil for stereolithography, ACS Applied Polymer Materials 2 (2020) 949–957. https://doi:10.1021/acsapm.9b01143.
[5] J.T. Sutton, K. Rajan, D.P. Harper, S.C. Chmely, Lignin-containing photoactive resins for 3D printing by stereolithography, ACS Appl. Mater. Interfaces 10 (2018) 36456–36463, https://doi.org/10.1021/acsami.8b13031.
[6] L.U. Kim, J.W. Kim, C.K. Kim, Effects of molecular structure of the resins on the volumetric shrinkage and the mechanical strength of dental restorative composites, Biomacromolecules 7 (2006) 2680–2687, https://doi.org/10.1021/bm060453h.
[7] James W. Wydra, Christopher R. Fenoli, Neil B. Cramer, Jeffrey W. Stansbury, Christopher N. Bowman, Influence of small amounts of addition-fragmentation capable monomers on polymerization-induced shrinkage stress, J. Polym. Sci., Part A: Polym. Chem. 52 (2014) 1315–1321, https://doi.org/10.1002/pola.27120.
[8] E. Andrzejewska, Photopolymerization kinetics of multifunctional monomers, Prog. Polym. Sci. 26 (2001) 605–665, https://doi.org/10.1016/S0079-6700(01)00004-1.
[9] P.K. Shah, J.W. Stansbury, C.N. Bowman, Application of an addition–fragmentation-chain transfer monomer in di(meth)acrylate network formation to reduce polymerization shrinkage stress, Polym. Chem. 8 (2017) 4339–4351, https://doi.org/10.1039/C7PY00702G.
[10] J.W. Ringsberg, A.Y.J. Ulfvarson, On mechanical interaction between steel and coating in stressed and strained exposed locations, Mar. Struct. 11 (1998) 231, https://doi.org/10.1016/S0951-8339(98)00015-X.
[11] N.B. Cramer, J.W. Stansbury, C.N. Bowman, Recent advances and developments in composite dental restorative materials, J. Dent. Res. 90 (2011) 402–416, https://doi.org/10.1177/0022034510381263.
[12] J.L. Ferracane, Resin composite–state of the art, Dent. Mater. 27 (2011) 29–38, https://doi.org/10.1016/j.dental.2010.10.020.
[13] L.F. Francis, A.V. McCormick, D.M. Vaessen, Effects of phase separation on stress development in polymeric coatings, J. Mater. Sci. 37 (2002) 4717–4731, https://doi.org/10.1016/S0032-3861(02)00042-3.
[14] R.R. Moraes, J.W. Garcia, M.D. Barros, S.H. Lewis, C.S. Pfeifer, J.C. Liu, J. W. Stansbury, Control of polymerization shrinkage and stress in nanogel-modified monomer and composite materials, Dent. Mater. 27 (2011) 509–519, https://doi.org/10.1016/j.dental.2011.01.006.
[15] S. Ye, S. Azarnoush, I.R. Smith, N.B. Cramer, J.W. Stansbury, C.N. Bowman, Using hyperbranched oligomer functionalized glass fillers to reduce shrinkage stress, Dent. Mater. 28 (2012) 1004–1011, https://doi.org/10.1016/j.dental.2012.05.003.
[16] A.J. Feilzer, A.J. Degee, C.L. Davidson, Quantitative determination of stress reduction by flow in composite resin restorations, Dent. Mater. 6 (1990) 167–171, https://doi.org/10.1177/00220345840630121101.
[17] H. Lu, J.W. Stansbury, C.N. Bowman, Impact of curing protocol on conversion and shrinkage stress, J. Dent. Res. 84 (2005) 822–826, https://doi.org/10.1177/154405910508400908.
[18] N. Silikas, G. Eliades, D.C. Watts, Light intensity effects on resin-composite degree of conversion and shrinkage strain, Dent. Mater. 16 (2000) 292–296, https://doi.org/10.1016/s0109-5641(00)00020-8.
[19] Jinlian Hu, Advances in Shape Memory Polymers, Woodhead Publishing, 2013.
[20] D. Habault, H. Zhang, Y. Zhao, Light-triggered self-healing and shape-memory polymers, Chem. Soc. Rev. 42 (2013) 7244–7256, https://doi.org/10.1039/C3CS35489J.
[21] S. Billiet, X.K.D. Hillewaere, R.F.A. Teixeira, F.E. Du Prez, Chemistry of crosslinking processes for self-healing polymers, Macromol. Rapid Commun. 34 (2012) 290–309, https://doi.org/10.1002/marc.201200689.
[22] Christopher J. Kloxin, Timothy F. Scott, Brian J. Adzima, Christopher N. Bowman, Covalent adaptable networks (CANs): a unique paradigm in cross-linked polymers, Macromolecules 43 (6) (2010) 2643–2653, https://doi.org/10.1021/ma902596s.
[23] Wim Denissen, Johan M. Winne, Filip E. Du Prez, Vitrimers: permanent organic networks with glass-like fluidity, Chem. Sci. 7 (2016) 30–38, https://doi.org/10.1039/c5sc02223a.
[24] Jon M. Matxain, José M. Asua, Fernando Ruipérez, Design of new disulfide-based organic compounds for the improvement of self-healing materials, Phys. Chem. Chem. Phys. 18 (2016) 1758–1770, https://doi.org/10.1039/C5CP06660C.
[25] G.C. Tesoro, V. Sastri, Reversible crosslinking in epoxy resins. I. Feasibility studies, J. Appl. Polym. Sci. 39 (1990) 1425–1437, https://doi.org/10.1002/app.1990.070390702.
[26] V.R. Sastri, G.C. Tesoro, Reversible crosslinking in epoxy resins. II. New approaches, J. Appl. Polym. Sci. 39 (1990) 1439–1457, https://doi.org/10.1002/app.1990.070390703.
[27] Aromatic disulfide crosslinks in polymer systems: Self-healing, reprocessability, recyclability and more Itxaso Azcune, Ibon Odriozola. https://doi.org/10.1016/j.eurpolymj.2016.09.023.
[28] Fengtao Zhou, Zijian Guo, Wenyan Wang, Xingfeng Lei, Baoliang Zhang, Hepeng Zhang, Qiuyu Zhang, Preparation of Self-Healing, Recyclable Epoxy Resins and Low-Electrical Resistance Composites Based on Double-Disulfide Bond Exchange, vol. 167, 2018, pp. 79–85, https://doi.org/10.1016/j.compscitech.2018.07.041.
[29] W.C. Oliver, G.M. Pharr, An improved technique for determining hardness and elastic modulus using load and displacement sensing indentation experiments, J. Mater. Res. 7 (1992) 1564–1583, https://doi.org/10.1557/JMR.1992.1564.
[30] I. E Ruyter, S. A Svendsen, Remaining methacrylate groups in composite restorative materials, Acta Odontol. Scand. 36 (1978) 75–82, https://doi.org/10.3109/00016357809027569.
[31] S.H. Dickens, J.W. Stansbury, K.M. Choi, C.J.E. Floyd, Photopolymerization kinetics of methacrylate dental resins, Macromolecules 36 (2003) 6043–6053, https://doi.org/10.1021/ma021675k.
[32] L.G. Lovell, J.W. Stansbury, D.C. Syrpes, C.N. Bowman, Effects of composition and reactivity on the reaction kinetics of dimethacrylate/dimethacrylate copolymerizations, Macromolecules 32 (1999) 3913–3921, https://doi.org/10.1021/MA990258D.
[33] M. I, BARSZCZEWSKA-RYBAREK Acta of Bioengineering and Biomechanics 19 (No. 1) (2017), https://doi.org/10.5277/ABB-00590-2016-01.
[34] N.G. McCrum, C.P. Buckly, C.B. Backnall, Principles of Polymer Engineering, Oxford Science Publications, London, 1997.